Supplementary Information: Relaxation of Stationary States on a Quantum Computer Yields a Unique Spectroscopic Fingerprint of the Computer's Noise

Scott E. Smart[1], Zixuan Hu[2], Sabre Kais[2], and David A. Mazziotti[1*]

Department of Chemistry and The James Franck Institute,
The University of Chicago, Chicago, IL 60637 USA and
Department of Chemistry, Department of Physics, and Birck Nanotechnology Center,
Purdue University, West Lafayette, IN, 47907 USA

(Dated: December 6, 2021)

Contents

* damazz@uchicago.edu

Supplementary Note I: Alternative single-qubit Hamiltonians

As mentioned in the main text, we also looked at other single-qubit Hamiltonians, namely $H_0 = \omega\sigma_x$ and $H_0 = \omega\sigma_y$, with the results in Supplementary Figure 1. For the σ_x and σ_y simulations, the higher frequency ($\omega = 0.5$) appears to be more noisy, which might be due to increased variances in measurement noise, or a systematic error in a frame rotation. Regardless, a somewhat stationary oscillating behavior is observed for the higher frequency, whereas the lower frequency ($\omega = 0.1$) is 'pushed' towards the center of the Bloch sphere. Scans of these trajectories also revealed similar trends, although we did not obtain as detailed data as in Figure 1 in the main text.

Supplementary Figure 1. Different trajectories for two frequencies, $\omega = 0.5$ (blue) and $\omega = 0.1$ (green), with three varying Hamiltonians: (a) $H_0 = \omega\sigma_x$; (b) $H_0 = \omega\sigma_y$, and; (c) $H_0 = \omega\sigma_z$. Points were taken after 5 gate applications with each gate equal to $\tau = 1/3$.

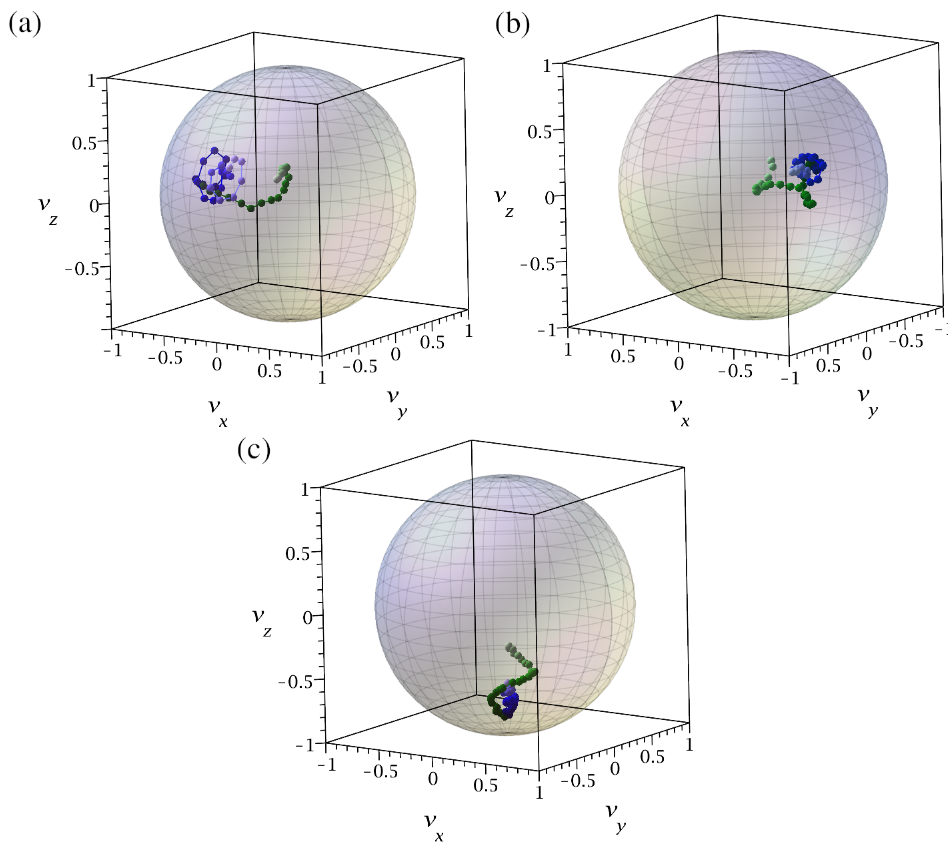

A. Comparison with T_1 relaxation times.

Looking at individual quantum devices, in some instances we see a linear relation between the simulated T_1 times, and the device T_1 times. While we expect this to be the case for uniform systems, in some instances gate errors could be uniquely worse than corresponding qubit coherence times (which becomes more commonplace with multi-qubit gates). We give an example in Supplementary Figure 2, where we compare the relaxation of the ibmqbogota qubit system, and the simulated quantum system. Note, while one can perform parallel measurements of the T_1 times, we found parallel simulation of the local qubit Hamiltonians introduced significant cross-qubit interactions, and so each relaxation time was measured separately.

Supplementary Figure 2. T_1 times for the simulated system (vertical axis, unitless), and the ibmqbogota device. For the simulated system, the $\exp[i\tau\hat{H}]$ operator was implemented 600 times, where $\hat{H} = \sigma_z$ ($\omega = 1$). 2^{11} measurements were taken for each experiment.

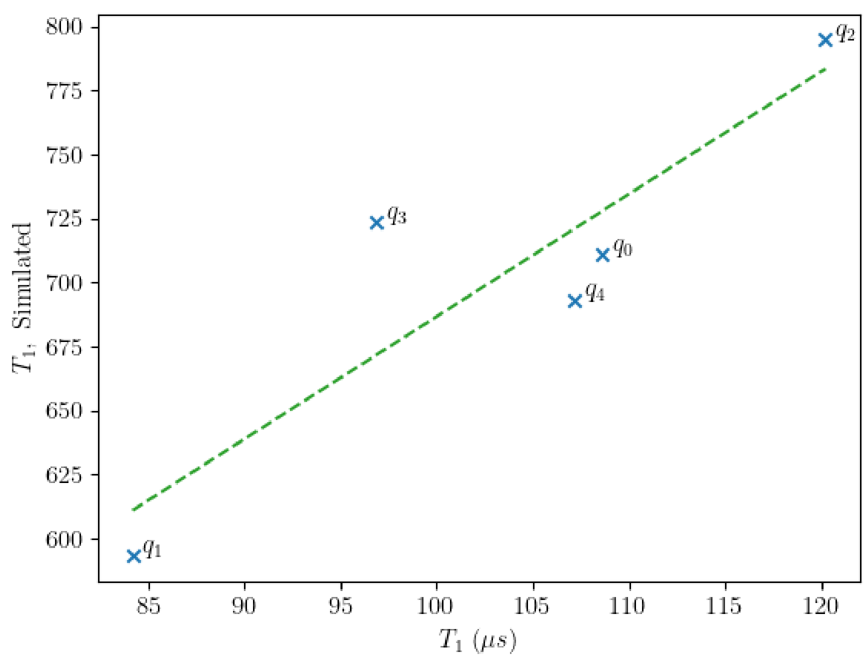

Supplementary Note II: Quantum Device Specifications

For the quantum computations we use variety of devices provided through the IBM Quantum Experience. The particular results reported here were performed on ibmq armonk (single-qubit results) and ibmq rome. The devices use fixed-frequency transmon qubits with co-planer waveguide resonators [1, 2], and the Python package Qiskit (v 0.15.0, 0.17.1) [3] were used to interface with the device. Device properties can be found in Supplementary Tables I - VI.

In particular, we report the qubit frequency, errors in the U_2 and U_3 gates, as well as readout errors, and T_1 and T_2 qubit times. For connected devices we include data on the CNOT gates as well. While preparing this draft, the basis set of operations changed to $\sqrt{X}$ and R_z gates, and so where appropriate we report the given performance of these gates.

Supplementary Table I. Calibration data for ibmq armonk taken over several days. Figure 1 and 2 were generated using data from 09-18-20, and Figure 3 and Supplementary Figure 1 were measured between 11-12-20 and 11-13-20.

Date	**Frequency**	$\mathbf{U}_2$	$\mathbf{U}_3$	$\mathbf{RO}_{0\|1}$	$\mathbf{RO}_{1\|0}$	$\mathbf{T}_1$	$\mathbf{T}_2$
	GHz	10^{-4}	10^{-4}	10^{-2}	10^{-2}	μs	μs
09-18-20	4.974	7.1	14.3	4.9	6.1	193.4	202.0
11-12-20	4.974	6.4	12.7	5.5	4.4	157.5	222.6
11-13-20	4.974	5.0	10.0	4.8	3.9	157.9	190.0

Supplementary Table II. Calibration from IBMQ Rome on 11-17-2020, used to generate Figure 4 in the main text.

Qubit	**Frequency**	$\mathbf{U}_2$	$\mathbf{U}_3$	$\mathbf{RO}_{0\|1}$	$\mathbf{RO}_{1\|0}$	$\mathbf{T}_1$	$\mathbf{T}_2$	$[j]$ $\mathbf{CNOT}_i^j$ (gate length)
i	GHz	10^{-4}	10^{-4}	10^{-2}	10^{-2}	μ s	μ s	10^{-2} (ns)
0	4.969	2.5	4.9	2.5	0.4	68.9	76.3	[1] 0.7 (320)
1	4.770	2.7	5.4	4.0	3.0	86.6	65.9	[0] 0.7 (356)

Supplementary Table III. Calibration data from ibmq-bogota, taken on 09-16-2021. See Figure 6 in the main text.

Qubit	**Frequency**	$\sqrt{X}$	X	$\mathbf{RO}_{0\|1}$	$\mathbf{RO}_{1\|0}$	$\mathbf{T}_1$	$\mathbf{T}_2$	$[j]$ $\mathbf{CNOT}_i^j$ (gate length)
i	GHz	10^{-4}	10^{-4}	10^{-2}	10^{-2}	μ s	μ s	10^{-2} (ns)
0	5.000	1.6	1.6	2.6	1.0	102.2	123.4	[1] 0.8 (690)
1	4.850	2.3	2.3	2.2	2.0	81.4	75.2	[0] 0.8 (654) [2] 0.9 (498)
2	4.783	2.1	2.1	2.6	0.7	78.1	115.5	[1] 0.9 (533) [3] 3.5 (341)
3	4.858	3.1	3.1	1.8	0.5	90.5	148.7	[2] 3.5 (306) [4] 0.8 (370)
4	4.978	1.5	1.5	4.2	0.9	98.4	171.2	[3] 0.8 (334)

Supplementary Table IV. Single-qubit calibration data from ibm devices, taken on 09-18-2021. See Figure 3 in the main text.

Backend	**Qubit**	**Frequency**	$\sqrt{X}$	X	$\mathbf{RO}_{0\|1}$	$\mathbf{RO}_{1\|0}$	$\mathbf{T}_1$	$\mathbf{T}_2$
i	GHz	10^{-4}	10^{-4}	10^{-2}	10^{-2}	μ s	μ s	10^{-2} (ns)
armonk	0	4.972	1.9	1.9	3.3	2.5	166.4	188.5
belem	0	5.090	1.6	1.6	8.0	6.4	104.2	115.4
	1	5.245	7.0	7.0	13.7	4.7	103.6	61.4
	2	5.361	2.5	2.5	2.9	1.0	98.6	33.4
	3	5.170	5.6	5.6	7.1	1.2	83.7	36.4
	4	5.258	3.6	3.6	3.7	0.9	90.3	135.3
bogota	0	5.000	1.7	1.7	1.8	1.4	104.9	136.2
	1	4.850	2.3	2.3	2.3	1.3	77.3	69.4
	2	4.783	1.9	1.9	2.3	0.6	118.5	186.3
	3	4.858	3.0	3.0	2.7	0.4	95.4	162.3
	4	4.978	1.4	1.4	2.7	1.5	104.0	190.7
casablanca	0	4.822	2.4	2.4	4.0	1.5	41.1	37.5
	1	4.760	2.3	2.3	3.5	0.8	34.7	79.2
	2	4.906	3.4	3.4	5.1	3.5	100.2	235.9
	3	4.879	3.0	3.0	2.2	0.9	73.7	143.6
	4	4.871	2.6	2.6	3.8	1.4	89.0	67.6
	5	4.964	1.8	1.8	1.7	0.7	88.8	172.1
	6	5.177	3.9	3.9	5.3	1.5	72.9	68.5

Supplementary References

[1] J. Koch, T. M. Yu, J. Gambetta, A. A. Houck, D. I. Schuster, J. Majer, A. Blais, M. H. Devoret, S. M. Girvin, and R. J. Schoelkopf, Charge-insensitive qubit design derived from the Cooper pair box, Phys. Rev. A **76**, 042319 (2007).

[2] J. M. Chow, A. D. Córcoles, J. M. Gambetta, C. Rigetti, B. R. Johnson, J. A. Smolin, J. R. Rozen, G. A. Keefe, M. B. Rothwell, M. B. Ketchen, and M. Steffen, Simple all-microwave entangling gate for fixed-frequency superconducting qubits, Phys. Rev. Lett. **107**, 080502 (2011).

[3] H. Abraham, AduOffei, R. Agarwal, I. Y. Akhalwaya, G. Aleksandrowicz, T. Alexander, M. Amy, E. Arbel, Arijit02, A. Asfaw, A. Avkhadiev, C. Azaustre, AzizNgoueya, A. Banerjee, A. Bansal, P. Barkoutsos, G. Barron, G. S. Barron, L. Bello, Y. Ben-Haim, D. Bevenius, A. Bhobe, L. S. Bishop, *et al.*, Qiskit: An open-source framework for quantum computing (2019).